

Electronic Supplementary Information (ESI) for “Electrochemical Li-ion storage in defect spinel iron oxides: The critical role of cation vacancies”

Benjamin P. Hahn[†], Jeffrey W. Long^{†*}, Azzam N. Mansour,[‡]
Katherine A. Pettigrew^{†,§}, Michael S. Osofsky[‡], and Debra R. Rolison^{†*}

*Naval Research Laboratory,
†Surface Chemistry Branch (Code 6170)
‡Materials and Sensors Branch (Code 6360)
Washington, DC 20375*

[‡]*Naval Surface Warfare Center–Carderock Division
Systems and Materials for Power and Protection Branch (Code 6160)
West Bethesda, MD 20817*

Assessment of other materials properties (surface area, conductivity, magnetism).

Brunaeur–Emmett–Teller (BET) surface areas were calculated from N₂-sorption experiments using a Micromeritics ASAP2010 Accelerated Surface Area and Porosimetry System. Prior to analysis, the ferrites were outgassed under vacuum at 150 °C for at least 24 h. The conductivity of the ferrite materials was estimated from two-point resistance measurements in which the ferrite powders were pressed into 7.3-mm circular discs that were sandwiched between two flat Pt surfaces for electrical resistance readings (Fluke 179 True RMS multimeter). Field-cooled and zero-field cooled magnetization data were obtained in a 100 Oe field (Magnetic Property Measurement System (MPMS) SQUID magnetometer) for temperatures between 300 K and 10 K. The magnetization of the samples was also studied as a function of the applied magnetic field (hysteresis loops) at 10 K and 300 K.

* Corresponding authors: Fax 202-767-3321; E-mail addresses: jeffrey.long@nrl.navy.mil, rolison@nrl.navy.mil.
§ Contract research scientist with Nova Research, Inc.; 1900 Elkin Street, Suite 230; Alexandria, VA 22308.

Supplemental Tables

Spinel Ferrite	Electronic Conductivity (S cm^{-1}) ^a	Surface Area ($\text{m}^2 \text{ g}^{-1}$) ^b	Saturation Magnetization (emu g^{-1}) ^c	XRD Particle Size (nm) ^d	TEM Particle Size (nm) ^e
$\text{Fe}_{3-x}\text{O}_4$	10^{-8}	55	59 ± 3	15–18	20 ± 10
Mo-ferrite	10^{-8}	152	11 ± 3	21–27	N/A

^a Rough estimates derived from two-point conductivity measurements.

^b BET-determined averages. Measurements are within $\pm 5\%$.

^c SQUID determined averages at 300 K. Both saturation magnetization values are significantly lower than literature values reported for bulk Fe_3O_4 (92 emu g^{-1})^{SR1} and $\gamma\text{-Fe}_2\text{O}_3$ (74 emu g^{-1})^{SR2,SR3}.

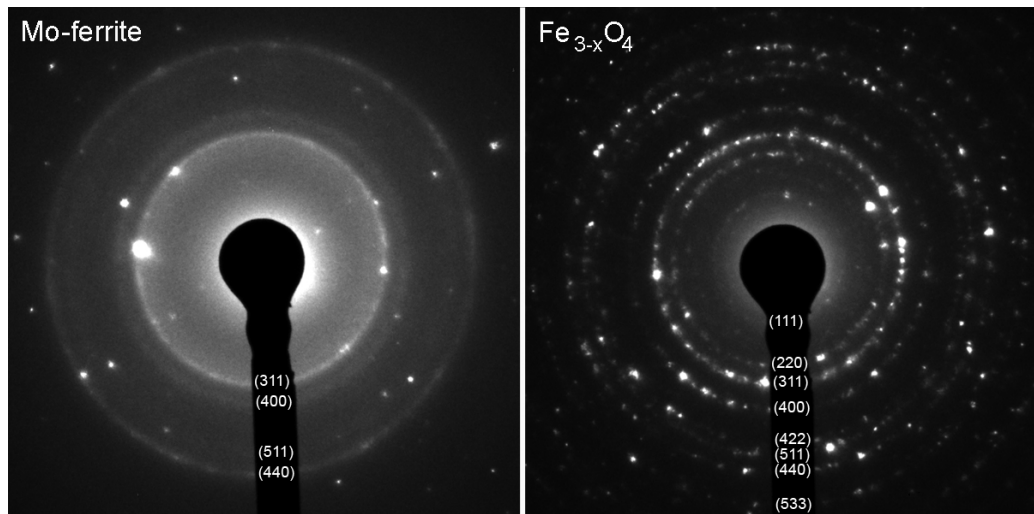
^d Scherrer analysis results from (220), (311), (400), (511), and (440) peaks.

^e Approximately 210 particles were measured for the $\text{Fe}_{3-x}\text{O}_4$ size distribution. The unique morphology of Mo-ferrite precludes a facile TEM determination of crystallite size; however, the scroll-like formations range in length from 26–70 nm with an average width of $5(\pm 3)$ nm.

Supplemental Table S1. Physical properties of $\text{Fe}_{3-x}\text{O}_4$ and Mo-ferrite.

Supplemental Figures

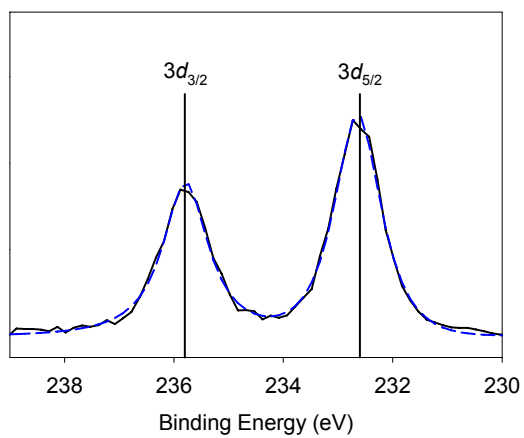
a



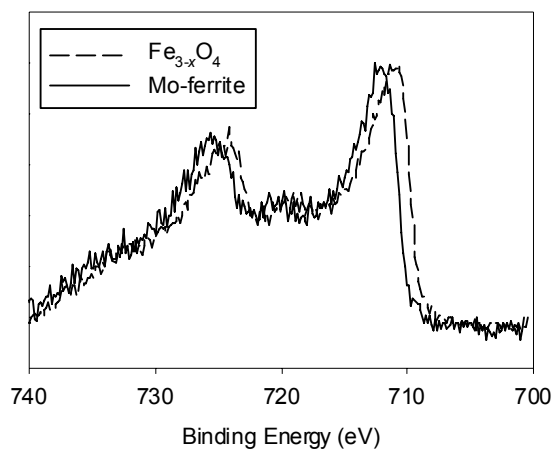
b

Mo-ferrite indexing		Fe _{3-x} O ₄ indexing	
(hkl)	d spacing (Å)	(hkl)	d spacing (Å)
(311)	2.49	(111)	4.85
(400)	2.13	(220)	2.87
(511)	1.60	(311)	2.47
(440)	1.45	(400)	2.05
		(422)	1.67
		(511)	1.58
		(440)	1.44
		(533)	1.24

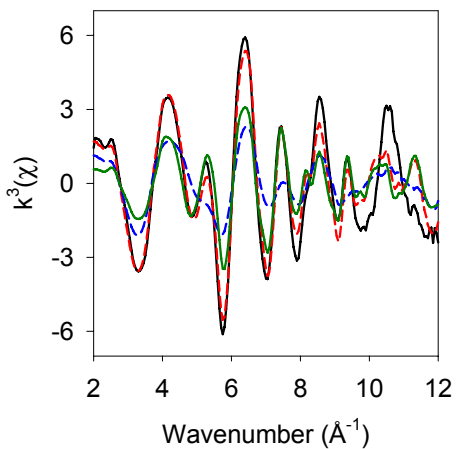
Supplemental Fig. S1. Electron diffraction (ED) indexing of the nanocrystalline structure. (a) ED patterns of Mo-ferrite and Fe_{3-x}O₄ acquired by transmission electron microscopy. (b) Lattice (hkl) and d-spacing assignments determined for the ring labels in (a).



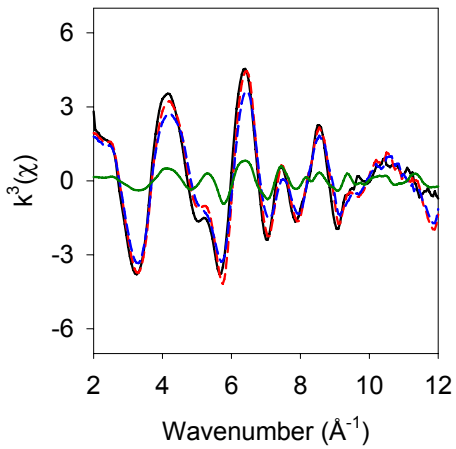
Supplemental Fig. S2. High-resolution X-ray photoelectron spectroscopy (XPS) of the Mo 3d region of Mo-ferrite. The background subtracted data (—) and fit (---) are shown. $\chi^2_{\text{red}} = 1.446$.



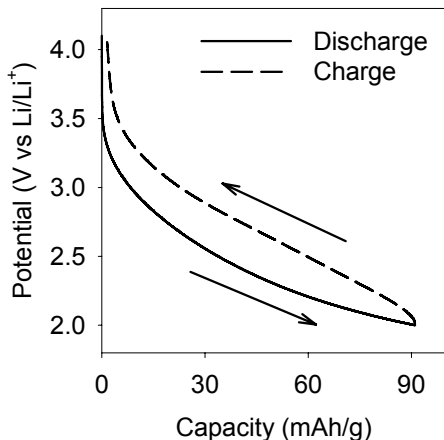
Supplemental Fig. S3. High-resolution X-ray photoelectron spectroscopy (XPS) of the Fe 2p region. Background subtracted XPS spectra are shown for $\text{Fe}_{3-x}\text{O}_4$ (---) and Mo-ferrite (—).



Supplemental Fig. S4. Linear combination of $k^3(\chi)$ for $\text{Fe}_{3-x}\text{O}_4$. The experimental data (—), fit data (----), and the amorphous FeOOH (---) and Fe_3O_4 (—) components of the fit are shown.
 $\chi^2_{\text{red}} = 0.752$.



Supplemental Fig. S5. Linear combination of $k^3(\chi)$ for Mo-ferrite. The experimental data (—), fit data (----), and the amorphous FeOOH (---) and Fe_3O_4 (—) components of the fit are shown.
 $\chi^2_{\text{red}} = 0.251$.



Supplemental Fig. S6. Charge-discharge plot of cycle #10 in Fig. 7b (working electrode contains Mo-ferrite) redrawn here to highlight the hysteresis. Electrolyte is 1 M LiClO₄/propylene carbonate and the applied current is 20 mA g⁻¹.

Supplemental References

-
- SR¹ M. Zhang, Q. Zhang, T. Itoh and M. Abe, *IEEE Trans. Magn.*, 1994, **30**, 4692.
SR² D. E. Speliotis, *J. Appl. Phys.*, 1967, **38**, 1207.
SR³ A. E. Berkowitz, W. J. Schuele and P. J. Flanders, *J. Appl. Phys.*, 1968, **39**, 1261.